A Journal of the Gesellschaft Deutscher Chemiker

Angewandte International Edition Chemie

GDCh

www.angewandte.org

Accepted Article

Title: Reactivity and Steric Parameters from 2D to 3D Bulky Pyridines : Increasing Steric Demand at Nitrogen with Chiral Azatriptycenes

Authors: Ali Bensaida, Damien Mahaut, Nikolay Tumanov, Johan Wouters, Benoît Champagne, Nicolas Vanthuyne, Raphaël Robiette, and Guillaume Berionni

To be cited as: *Angew. Chem. Int. Ed.* **2024**, e202407503

Link to VoR: https://doi.org/10.1002/anie.202407503

WILEY VCH

10.1002/anie.202407503

RESEARCH ARTICLE

WILEY-VCH

Reactivity and Steric Parameters from 2D to 3D Bulky Pyridines : Increasing Steric Demand at Nitrogen with Chiral Azatriptycenes

Ali Ben Saida,[a] Damien Mahaut,[a] Nikolay Tumanov,[a] Johan Wouters,[a] Benoît Champagne,[a] Nicolas Vanthuyne,[b] Raphaël Robiette,[c] Guillaume Berionni*[a]

[a] Dr. A. Ben Saida, Dr. D. Mahaut, Dr. N. Tumanov, Prof. J. Wouters, Prof. B. Champagne, Prof. G. Berionni
Department of Chemistry and Namur Institute of Structured Matter
Université de Namur
61 Rue de Bruxelles, 5000 Namur, Belgium
E-mail: guillaume.berionni@unamur.be

[b] Dr. N. Vanthuyne
Aix Marseille Univ, CNRS, Centrale Marseille, iSm2, Marseille, France

[c] Prof. R. Robiette
Institute of Condensed Matter and Nanosciences
Université catholique de Louvain
Place Louis Pasteur 1 Box L4.01.02, 1348 Louvain-la-Neuve, Belgium

Supporting information for this article is given via a link at the end of the document

Abstract: Sterically hindered pyridines embedded in a three-dimensional triptycene framework have been synthesized, and their resolution by chiral HPLC enabled access to unprecedented enantiopure pyridines exceeding the known steric limits. The design principles for new axially chiral pyridine derivatives are then described. To rationalize their associations with Lewis acids and transition metals, a comprehensive determination of the steric and electronic parameters for this new class of pyridines was performed. This led to the general parameterization of the steric parameters (percent buried volume %V_{Bur}, Tolman cone angle θ, and He_8_steric descriptor) for a large set of two- and three-dimensional pyridine derivatives. These parameters are shown to describe quantitatively their interactions with carbon- and boron-centered Lewis acids and were used to predict the ΔG° of association with the prototypical $B(C_6F_5)_3$ Lewis acid widely used in frustrated Lewis pair catalysis. This first parameterization of pyridine sterics is a fundamental basis for the future development of predictive reactivity models and for guiding new applications of bulky and chiral pyridines in organocatalysis, frustrated Lewis pairs, and transition-metal catalysis.

Introduction

Pyridines have found widespread uses as nucleophilic catalysts in organocatalysis,[1,2] as Lewis bases in frustrated Lewis pair chemistry (Scheme 1a),[3] and as ligands in transition-metal complexes used for organometallic catalysis (Scheme 1b).[4-6] Intense efforts have been devoted to embed the pyridine core in chiral frameworks, leading to the creation of ingenious designs based on central, axial, planar and helical chirality (Scheme 1c).[7-12] Although pyridines are attracting significant interest for the development of new catalysts and auxiliaries, it is surprising that steric and electronic parameters for these nitrogen containing heteroaromatics remain virtually unknown up to date.

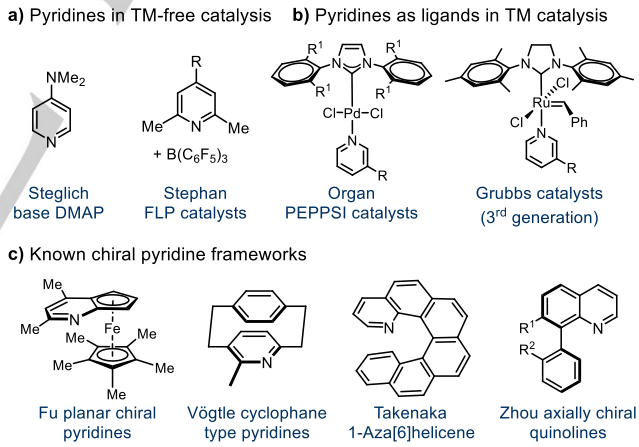

Scheme 1. Selected examples of pyridine used: a) in organocatalysis and frustrated Lewis pair (FLP) chemistry; b) in transition-metal (TM) catalysis and; c) selected examples of chiral and sterically-hindered pyridine derivatives.[7-12]

In comparison to phosphines and *N*-heterocyclic carbenes (NHCs), whose steric parameters such as Charton,[13] Sterimol,[14] Tolman cone angle,[15] buried volume,[16] He_8_steric[17] and topographic map[18] have been extensively used as predictive tools for the optimization and development of new catalysts,[16c,19] only a few steric descriptors have been reported for amines and pyridines.

Indeed, only the Tolman cone angles of a few amines used as ligands in Pd and Ni complexes,[20] and the boron-related cone angles of a couple of pyridines (pyridine and lutidine) have been determined so far.[21-23] Thus, there is to date no systematic parameterization of the steric hindrances or of the electronic

parameters of pyridines that has been reported, and the investigation of three-dimensional pyridine steric, electronics, and reactivity parameters remains largely unexplored.

As every catalyst involving the coordination of a pyridine to a Lewis acid or to a transition metal requires a subtle balance between Lewis basicity and steric hindrance,[3a,21,24] we started to expand the diversity of pyridine derivatives in terms of steric, electronic, and chiral properties by designing new sterically encumbered chiral pyridines embedded in a three-dimensional triptycene framework.

We also took advantage of the triptycene tricyclic scaffold to design bulky pyridines surpassing the size of the bulkiest pyridines known so far.[25] In these rigid 3D aromatic systems, we could fine-tune with great accuracy the environment of the nitrogen atom by functionalizing the triptycene scaffold at three strategic positions, imposing three substituents pointing inside the nitrogen atom coordination sphere. This enabled us to expand the stereo-electronic limits of pyridine derivatives and to introduce unprecedented central and axial chiralities thanks to the original triptycene tricyclic cage-shaped structure (Figure 1).[26]

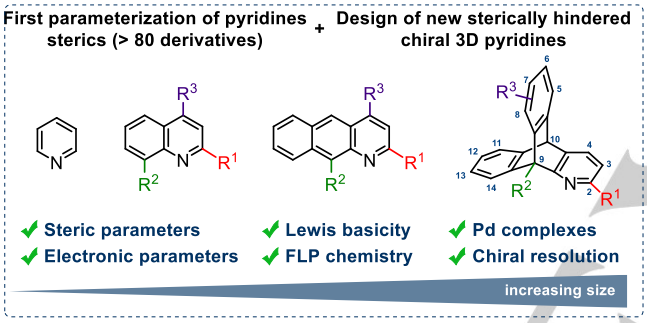

Figure 1. This work : parameterization of pyridine sterics and design of new class of chiral pyridine derivatives with triple control of the coordination sphere.

Results and Discussion

Synthesis, Structural Sharacterization and First Chiral Resolution of Azatriptycenes

As per our interest in the unique triptycene scaffold composed of three aromatic rings linked by a bicyclo[2.2.2]octane motif, we synthesized a series of 1-azatriptycenes **1-14**. Inspired by Markgraf's pioneer work on preparing the parent 1-azatriptycene **1**,[27] we have now greatly expanded the reaction scope as our synthetic approach involves the synthesis of several functionalized benzo[g]quinoline precursors (detailed procedures described in the SI), followed by a [4+2] cycloaddition with an excess of *in-situ* generated mono, di, and tetra-substituted benzynes (Scheme 2).

Efficient and expeditious Cl/Li exchange between *n*BuLi and 9-chloroazatriptycenes followed by hydrolysis is employed rather than the classical homolytic C-Cl cleavage and hydrogen atom transfer with trialkyltin hydride R_3SnH. Such Cl/Li exchange with *n*BuLi is rarely observed,[28] and is presumably due to the proximity of the pyridine nitrogen atom, which assists in directing the alkyl-lithium reagent via the complex-induced proximity effect.[29]

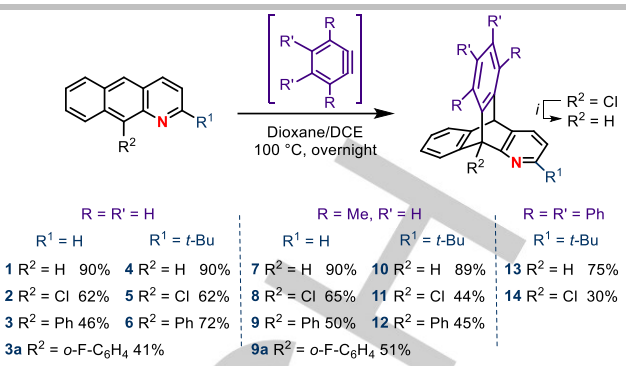

Scheme 2. Synthesis of the sterically hindered 1-azatriptycenes **1-14**. Conditions: i) *n*BuLi, Et_2O, -94 °C to r.t., 2 h, then H_2O. See details in SI.

These unprecedented chiral azatriptycenes derivatives **7-14** were resolved for the first time by semi-preparative chiral HPLC, giving access to a series of enantiopure chiral pyridines. As an example, the resolution of both enantiomers of chiral azatriptycene **11** (Figure 2a) by chiral HPLC at a scale of 100 mg, resulted in *ee*'s > 98.5 %. The first and second eluted enantiomers were distinguished based on their solid-state structures (Figure 2b) and exhibited opposite specific rotation $[\alpha]_{405}^{25}$ of ± 10° (CH_2Cl_2, c = 0.5) and typical mirror-image ECD spectra.

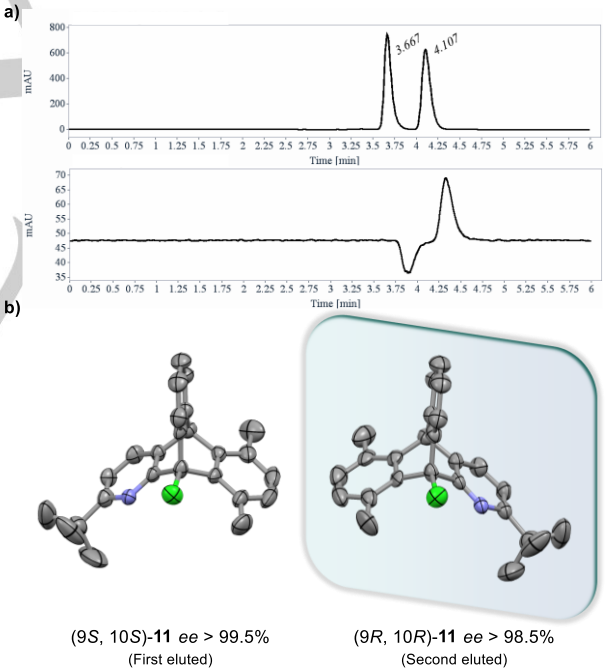

Figure 2. a) Representative chromatograms for resolution of compound **11**, chromatographic conditions: Lux-Cellulose-4 (250 x 4.6 mm), mobile phase hexane / 2-PrOH (95:5), flow-rate = 1 mL/min, UV detection at 230 nm (top) and circular dichroism detector at 254 nm (bottom); b) Structures of both enantiomers of **11** in the solid state (50% probability ellipsoids representation).

Interestingly, the X-ray structures of **3a, 9a,** and **12** show that the aryl groups in the 9-position align parallelly with the pyridine ring, leading to an unusual C-H···N intramolecular interaction. This interaction results in an unusually deshielded broad signal at 10.17 ppm in the ^{1}H NMR spectrum for one of the *ortho*-hydrogens on the central aromatic ring of compound **12**, while the other *ortho*-hydrogen displays a signal at 7.43 ppm.

This broad signal in the ^{1}H NMR spectrum, with a large chemical shift difference of nearly $\Delta\delta \approx 3$ ppm for the hydrogen located in the *ortho*-position of the aryl ring, is also observed in **3a** (δ = 10.36 ppm), **9** (δ = 9.88 ppm) and **9a** (δ = 10.19 ppm). This suggests restricted rotation at the C_9-C_{Ar} bond connecting the aryl ring and the triptycene core (Figure 3). Thus, one can expect atropisomerism along the Csp^3-Csp^2 bond in the case of **9a** which combines an *o*-F on the aryl group in the 9-position and a methyl group in the *ortho*-position of one aromatic group of the triptycene structure, enabling it to stop rotation and reach new axially chiral pyridines.

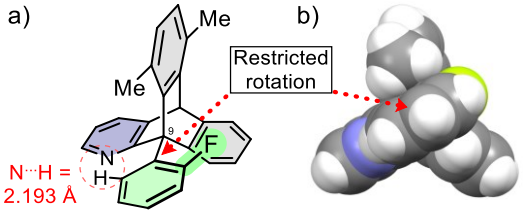

Figure 3. a) Stucture and b) space-fill model of the solid-state structure of **9a** showing the intramolecular N···H interaction and the restricted rotation at the C-C bond connecting the position 9 of triptycene and the *o*-F-C_6H_4 substituent.

Accordingly, we have conducted further examination of the conformational equilibrium of these 9-arylazatriptycenes. To evaluate the influence of the *ortho*-fluorine and *ortho*-methyl groups on this equilibrium, we have computed the energy profiles for rotation around the C_9-C_{Ar} bond in compounds **3a**, **9**, and **9a** (see SI). Our calculations indicated that, in all three cases, the most stable conformer shows the aryl ring aligned parallel to the pyridine ring, consistent with X-ray diffraction and ^{1}H NMR analysis (see Figure 3 and SI). Additionally, rotation barriers arising from steric repulsions were found to be 11.5 kcal mol^{-1} for **3a** and 17.8 kcal mol^{-1} for **9**, demonstrating that steric interactions induced by a single *o*-F or *o*-Me substituent do not prevent a rapid conformational equilibrium. Calculations of the full rotation profile for **9a** (Figure 4) revealed a free energy barrier maxima of 27.0 kcal mol^{-1}, indicating that the combination of the *o*-F substituent on the rotating aromatic ring and the *o*-Me substituent on the azatriptycene scaffold results in a frozen rotation and stable atropisomerism.

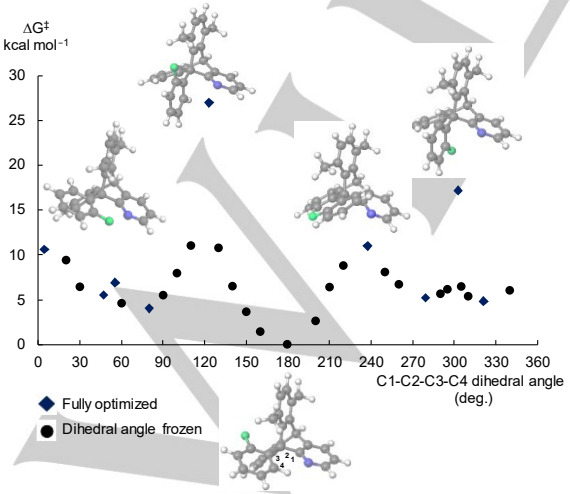

Figure 4. Computed structure of **9a** and corresponding conformers and rotation transition states. Free energy barriers of rotation in kcal mol^{-1} based on M06-2X/6-311+(d,p)//BP86/6-31G(d) calculations.

Coordination Chemistry of Azatriptycenes

Because of its rigid benzotricyclic structure, we hypothesized that the triptycene framework could provide precise control over the steric and electronic properties of the pyridine ring in **1**-**14**.

We thus investigated the association of azatriptycenes, spanning from those with minimal steric hindrance (*e.g.*, compound **1**) up to the most bulky substituted at positions 2, 8, and 9 (*e.g.,* compound **12**), with carbenium ions, boron Lewis acids, and their coordination with palladium for forming Pd-NHCs PEPPSI type complexes (Scheme 3 and Figure 5).

While the smallest azatriptycene **1** readily associates with the tris(pentafluorophenyl)borane ($B(C_6F_5)_3$) boron Lewis acid and with the $PdCl_2$ precursor, the more sterically hindered azatriptycenes **4** and **5** do not associate with $B(C_6F_5)_3$; the system being predominantly dissociated. This results in the formation of a series of frustrated Lewis pairs that enable the cleavage of H_2 and H_2O activation.

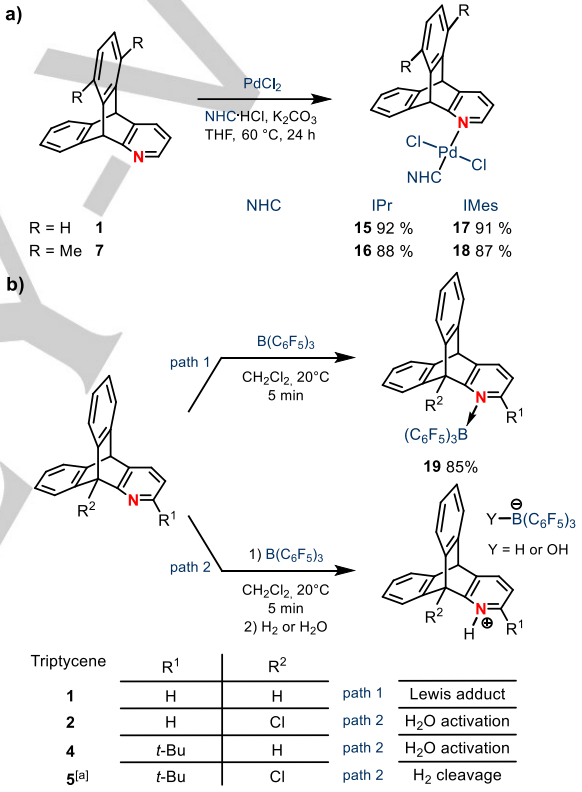

Triptycene	R^1	R^2		
1	H	H	path 1	Lewis adduct
2	H	Cl	path 2	H_2O activation
4	*t*-Bu	H	path 2	H_2O activation
5[a]	*t*-Bu	Cl	path 2	H_2 cleavage

Scheme 3. a) Formation of Pd complexes **15**-**18**, with IPr = 1,3-bis(2,6-diisopropylphenyl)imidazol-2-ylidene and IMes = 1,3-Bis(2,4,6-trimethylphenyl)imidazol-2-ylidene; b) Formation of the Lewis adduct **19** and H_2 or H_2O activation; [a] heterolytic splitting of H_2, conditions : H_2 10 bar, CH_2Cl_2, r.t., overnight, ^{11}B NMR of the pyridinium hydridoborate salt δ (^{11}B) = -26.6 ppm, d, $^1J_{B\text{-}H}$ = 73 Hz.

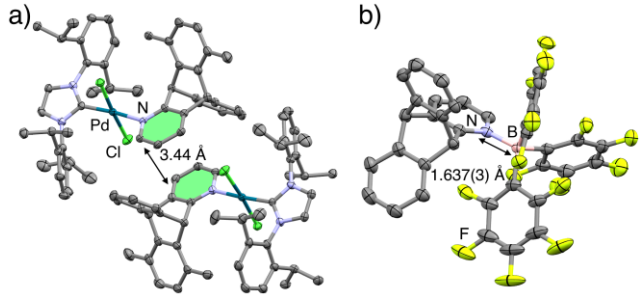

Figure 5. Molecular structures showing a) the antiparallel π-stacking interactions with distances of 3.455 Å in **16** and; b) structure of **19** in the solid state (50% probability ellipsoids representation for both).

Steric Parameters and Correlation Analysis

The difference in Lewis basicity between compounds **1** and **4** originates from differences in steric hindrance. For azatriptycenes with intermediate sizes, a quantitative parameterization of steric hindrance is necessary to be able to predict whether a covalent bond will form or if a frustrated Lewis pair will emerge with $B(C_6F_5)_3$.

This prompted us to determine three widely used steric parameters (percent buried volume $\%V_{Bur}$,[16] Tolman cone angle θ,[15] He_8_steric descriptor,[17] Figure 6) of a large set of 2D and 3D pyridines based on their X-ray structures and on their structures computed by quantum chemical calculations (see SI).

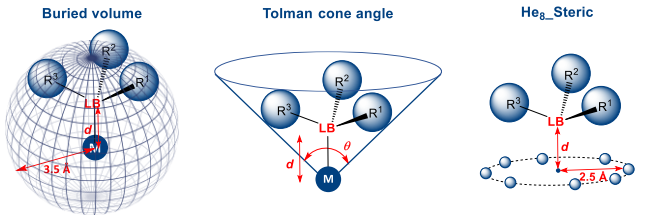

Figure 6. Schematic representation of percent buried volume ($\%V_{Bur}$), Tolman cone angle (θ) and helium steric descriptor (He_8_steric).

These values were determined considering two different distances, (i) 1.7 Å for evaluating the steric shielding of pyridines towards carbocations and Lewis acids,[21] in the context of organocatalysis, and more generally, in transition-metal free catalysis (*e.g.,* Lewis acid-base associations, main-group mediated and frustrated Lewis pairs catalysis), and (ii) 2.2 Å in order to investigate their steric properties in coordination with transition metals such as Pd, Ir, Ru, and Au (Table 1).[20a]

Since chemical behavior cannot be reduced to a single numerical value, the buried volume parameter is assessed in conjunction with a topographic steric map, which provides a three-dimensional representation of the ligand's shape from the perspective of the boron center. Even with high steric hindrance, these maps reveal significant free space along the y-axis, while the phenyl (**12**) and chlorine (**14**) groups in the x-axis half-plane contribute to stronger hindrance. The asymmetric environment is a result of the methyl and phenyl groups in the second ring of the triptycene, situated in the north-western and south-western quadrants, respectively (Figure 7).

Table 1. Computed buried volume $\%V_{Bur}$ [a,b,c], Tolman cone angle θ (in degrees) [a], and He_8_steric [d] (in kcal mol^{-1}) parameters for pyridine derivatives and 1-azatriptycenes in their uncomplexed form (see the SI for more details).

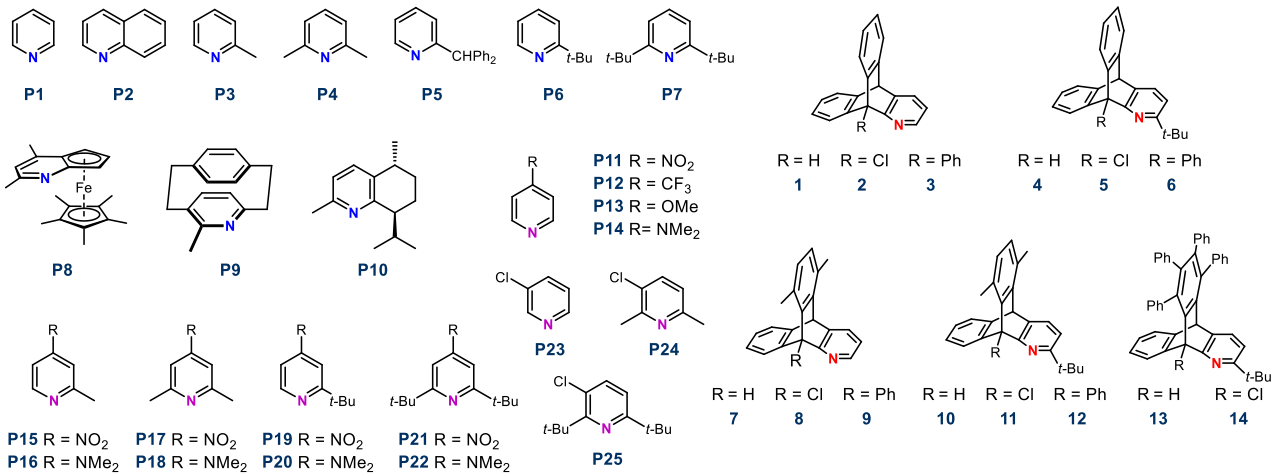

	P1	P2	P3	P4	P5	P6	P7	P8	P9	P10	1	2
$\%V_{Bur}$/ 1.7 Å	23.9	28.3	28.7	33.7	35.1	37.7	51.6	38.8	40.0	41.9	28.3	37.0
$\%V_{Bur}$/ 2.2 Å	18.4	22.1	22.5	26.8	28.5	31.3	44.3	30.4	31.6	35.0	21.8	30.7
θ/ 1.7 Å	140	156	158	173	181	183	221	188	194	205	161	187
θ/ 2.2 Å	109	123	125	144	156	156	197	163	166	178	137	170
He_8_steric / 1.7 Å	5.2	15.2	15.4	26.4	19.5	28.3	50.0	24.3	22.7	30.9	16.1	25.6
He_8_steric / 2.2 Å	1.6	4.7	5.5	10.7	6.1	12.0	27.7	9.2	8.1	13.3	4.6	10.1

	3	4	5	6	7	8	9	10	11	12	13	14
$\%V_{Bur}$/ 1.7 Å	46.5	44.2	52.3	61.4	30.0	37.8	-	44.5	52.2	62.2	-	54.5
$\%V_{Bur}$/ 2.2 Å	42.3	36.3	44.8	56.0	23.4	31.5	-	37.0	45.0	56.8	-	47.3
θ/ 1.7 Å	219	218	220	235	-	200	-	222	233	248	-	241
θ/ 2.2 Å	209	196	200	219	-	182	-	200	211	231	-	220
He_8_steric / 1.7 Å	28.3	41.2	46.9	50.1	15.3	26.0	30.5	42.1	45.9	57.0	42.9	48.0
He_8_steric / 2.2 Å	11.9	23.6	26.0	27.8	4.2	9.6	13.4	24.5	25.1	34.7	26.1	27.0

[a] Based on the fully optimized structures of pyridines **P1-P10** at the M06-2X/6-311G(d) (IEFPCM for CH_2Cl_2) level and on the solid-state structures for 1-azatriptycenes **1-14**. [b] The percent buried volume is determined using the SambVca 2.1 application. [c] The substituents in the meta or para position in **P11-P25** have a negligible effect on the buried volume, a modification of less than 0.1% of the $\%V_{Bur}$ parameter is observed (see SI). [d] Computed at the BP86/6-31G(d) level following the method of Fey et al.[17a]

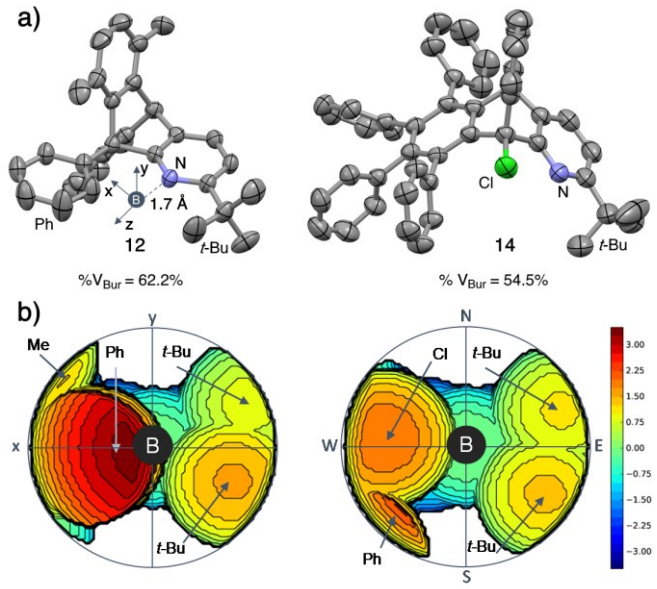

Figure 7. a) Structures of the most bulky chiral azatriptycenes **12** and **14** in the solid state (50% probability ellipsoids representation); b) topographic steric maps of **12** and **14** for B-N distance of 1.7 Å using the SambVca 2.1 application. The isocontour curves are in Å; the red and blue zones indicate the more- and less-hindered zones, respectively.

The steric parameters, θ, He$_8$_steric, and %V$_{Bur}$, for an M–N bond distance of 1.7 Å, are well correlating (Figure 8), indicating that they are appropriate for describing the steric effects of pyridines.

The correlation between %V$_{Bur}$ at 2.2 Å and %V$_{Bur}$ at 1.7 Å is also excellent, with a regression equation of Y = 0.9897 X – 6.028 (R^2 = 0.9936; see SI). Thus, substituents will be discussed on the basis of the most commonly used %V$_{Bur}$ steric descriptor. Of note, the %V$_{Bur}$ value of **6** is higher than expected from the correlations because the %V$_{Bur}$ value is calculated from the structure in the solid-state, where the phenyl group in the 9-position aligns perfectly parallel with the pyridine ring and shields the nitrogen atom. Thus, the conformational equilibrium associated with the rotation of the aryl groups in position 9 is not taken into consideration in the values for **3**, **6**, and **12**, which therefore deviate from the correlation line.

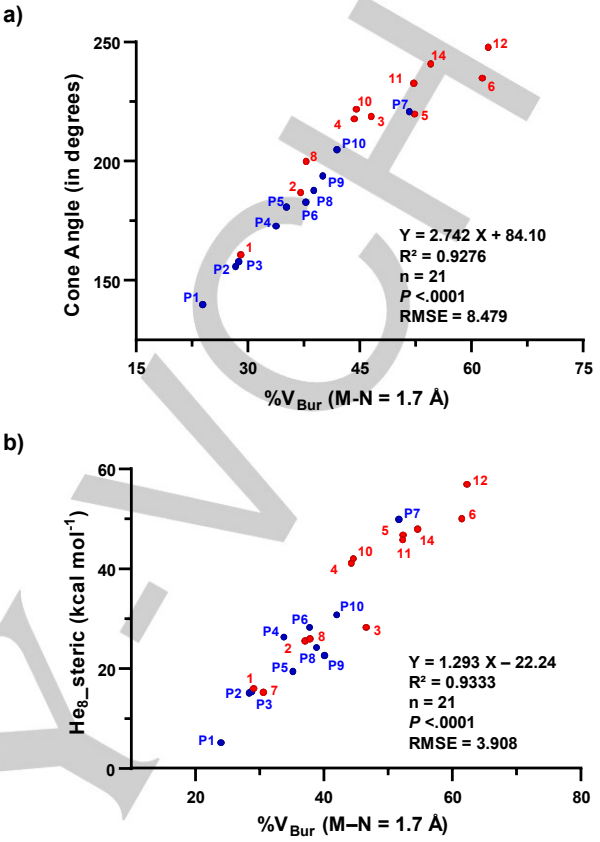

Figure 8. a) Correlation between the Tolman cone angle and the %V$_{Bur}$ parameters at 1.7 Å; b) correlation between the He$_8$_steric and the %V$_{Bur}$ parameters at 1.7 Å. Aryl-azatriptycene **3** was excluded from the linear regression analysis as the helium ring cannot be optimized perpendicularly to the pyridine axis. n = sample size, P = *p*-value, and RMSE = root-mean-square error.

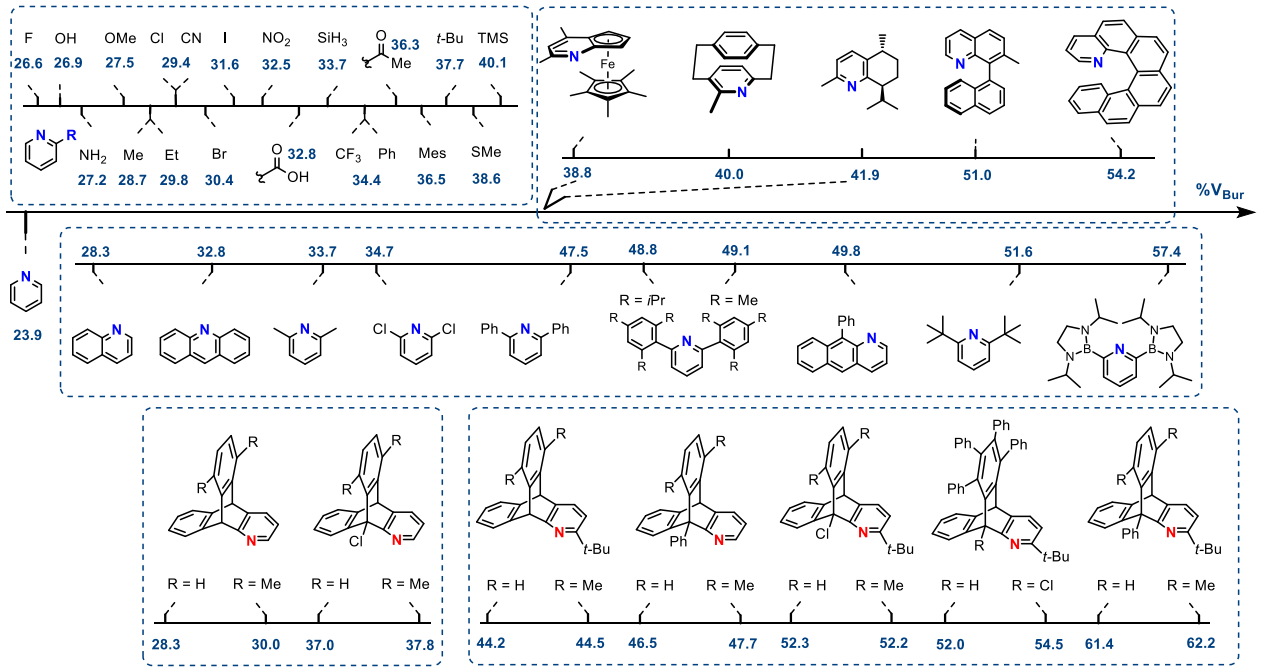

Figure 9. Computed buried volume %V$_{Bur}$ at 1.7 Å from the nitrogen for pyridine derivatives based on their solid-state structures extracted from the Cambridge Structural Database (CSD) (see the SI for more details).

The substituent effects on steric hindrance were deconvoluted by comparing the buried volume of the corresponding *ortho*-substituted pyridines to that of pyridine (%V_{Bur} = 23.9%), giving access to individual substituents steric effects (Table 2).[32]

Table 2. Percent buried volume increment values (Δ%V_{Bur}) for substituents in 2-substituted pyridines at a distance of 1.7 Å (see the SI for the determination of %V_{Bur} for the corresponding *ortho*-substituted pyridines).

Group	%V_{Bur}	Group	%V_{Bur}	Group	%V_{Bur}
F	2.7	allyl	6.0	CF_3	10.5
OH	3.0	Br	6.5	pyrrolyl	10.8
NH_2	3.3	SH	6.6	COMe	12.4
OMe	3.6	I	7.7	mesityl	12.6
vinyl	4.8	NO_2	8.6	N_3	13.7
Me	4.8	COOH	8.9	*t*-Bu	13.8
Cl	5.5	SiH_3	9.8	COCl	14.5
CN	5.5	Ph	10.5	SMe	14.7
Et	5.9	*p*-tolyl	10.5	TMS	16.2

The integration of the pyridine moiety in a triptycene scaffold induces an increase in steric hindrance by only Δ%V_{Bur} = 4.4 % (Figure 9). This effect is comparable to the hindrance created by an *ortho*-methyl substituent as well as the steric hindrance demonstrated in quinoline (%V_{Bur} = 28.3 for **1**, 23.9, 28.3, and 28.7 for **P1, P2,** and **P3**, respectively). The azatriptycenes featuring methyl groups on one aromatic ring **7-12** demonstrate a marginal increase in %V_{Bur} (Δ%V_{Bur} = 1.0%) when compared to their non-substituted analogues **1-6** (Figure 9).

This is due to the methyl group's positioning mostly outside the sphere, resulting in a minimal effect on steric hindrance. However, the azatriptycene structure enables the introduction of substituents in 9-position, which has a great impact on steric hindrance. Indeed, in *ortho*-substituted pyridines, the Δ%V_{Bur} effects of Cl and Ph are 5.5% and 10.5%, respectively, whereas in 9-substituted azatriptycenes, the %V_{Bur} is increased by 8.7% for the Cl atom and by 18.2% for the Ph group.

Furthermore, combining substituents at positions 2, 8 and 9 results in a huge increase in steric hindrance, leading to 1-azatriptycene **12** with a buried volume of up to 62.2% (Figure 9). This value exceeds by far the %V_{Bur} of the 2,6-di-*tert*-butylpyridine (%V_{Bur} = 51.6%) and the %V_{Bur} of the bulkiest pyridines known to date.[25] This leverages the unique architecture of triptycene as a versatile scaffold for introducing controlled steric hindrance, with %V_{Bur} ranging from 28 to 62%. The effect of sterics on Lewis basicity was next probed experimentally.

Lewis Basicity of Azatriptycenes

To assess the reactivity of azatriptycenes and compare it with planar 2D pyridine derivatives, we investigated the kinetics and thermodynamics of the association between the representative azatriptycene **7** and a diarycarbenium ion of known Lewis acidity parameter (*LA* = −6.33)[30] by UV-vis spectroscopy (Scheme 4).

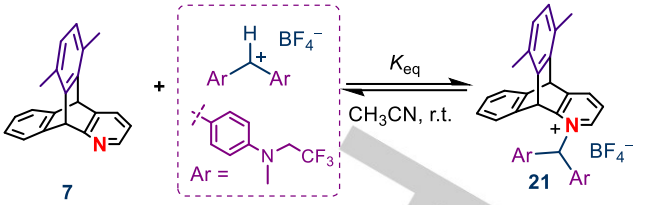

Scheme 4. Reversible association of **7** with a benzhydrylium ion in CH_3CN.

Even when using a large excess of **7** over the benzhydrylium ion, the binding of it's nitrogen atom with the carbenium center does not proceed to completion, and only a partial conversion and formation of **21** were observed by UV-Vis and NMR spectroscopy (see the SI), allowing for the determination of the equilibrium constant through binding titration analysis (K = 2.37 × 10^3 M^{-1}). The Lewis basicity of azatriptycene **7** is assessed using the Mayr equation (1)[31] giving a Lewis basicity parameter of 9.70, demonstrating similar Lewis basicity as *ortho*-substituted pyridines (Figure 10).

$$\log K\ (20\ °C) = LA + LB \qquad (1)$$

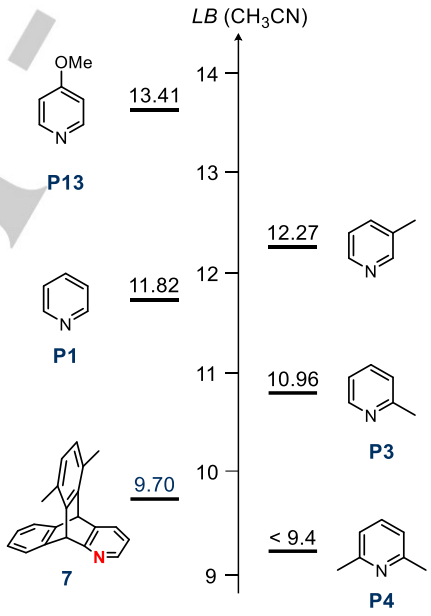

Figure 10. Lewis basicity of **7** in CH_3CN and comparative Lewis basicity scale with other pyridines (*LB* values from the literature[30,31]). For the determination of the nucleophilicity parameter of **7**, see the SI.

Quantum-Chemical Calculation of Electronic Parameters

The Brønsted and Lewis basicity of compounds **1–14** was evaluated alongside a larger series of mono- and bis-*ortho*-substituted pyridine derivatives **P1**-**P25** by computing their proton affinities (PA), methyl cation affinities (MCA), and Gibbs free energies associations ΔG^0 with $B(C_6F_5)_3$ as a prototypical boron Lewis acid (Table 3).

Table 3. Enthalpies of reaction of pyridines with H^+ (proton affinity, PA) and Gibbs free energies of complexation with CH_3^+ (methyl cation affinity, MCA) and with $B(C_6F_5)_3$ in kJ mol^{-1} based on M06–2X/6–311G(d) (IEFPCM for CH_2Cl_2) calculations (see the SI).

	P1	P2	P3	P4	P5	P6	P7	P8	P9	P10
PA	718	718	726	734	720	726	734	740	740	737
MCA	375	368	372	368	365	340	288	393	372	358
$\Delta G^0B(C_6F_5)_3$	-93	-78	-80	-26	-40	28	177	-68	-26	25
	P11	**P12**	**P13**	**P14**	**P15**	**P16**	**P17**	**P18**	**P19**	**P20**
PA	677	693	734	760	687	764	694	772	689	765
MCA	336	343	386	410	337	409	330	402	302	371
$\Delta G^0B(C_6F_5)_3$	-69	-73	-101	-117	-58	-86	-4	-52	36	-11
	P21	**P22**	**P23**	**P24**	**P25**	**1**	**2**	**3**	**4**	**5**
PA	687	766	695	710	710	716	706	709	721	712
MCA	247	317	351	342	246	369	324	327	327	276
$\Delta G^0B(C_6F_5)_3$	201	138	-78	-10	-	-94	-23	18	60	158
	6	**7**	**8**	**9**	**9a**	**10**	**11**	**12**	**13**	**14**
PA	732	717	710	709	690	722	716	707	719	714
MCA	302	370	325	327	302	328	276	273	325	276
$\Delta G^0B(C_6F_5)_3$	202	21	-13	46	60	72	164	210	63	164

In agreement with the computed ΔG^0 value of -94 kJ mol^{-1} for the association of 1-azatriptycene **1** with $B(C_6F_5)_3$, which is almost identical to the value for pyridine (-93 kJ mol^{-1}), we confirmed by NMR that the Lewis adduct **19** is formed spontaneously, and slow evaporation of the solution provided crystals suitable for X-ray diffraction analysis (Figure 5). On the opposite, no NMR signals corresponding to a Lewis adduct **20** were detected when mixing the strongly hindered azatriptycene **4** with $B(C_6F_5)_3$ in CD_2Cl_2, in line with the computed positive ΔG^0 value of +60 kJ mol^{-1} for the association with $B(C_6F_5)_3$.

As the proton affinities of this large range of azatriptycenes span a relatively small range of maximum 26 kJ mol^{-1} (PAs from 732 to 706 kJ mol^{-1}), we hypothesized that their association or not with the $B(C_6F_5)_3$ boron Lewis acid is mostly governed by their steric properties.

This is also supported by the good linear correlation between the Gibbs free energies of association ΔG^0 with $B(C_6F_5)_3$ and the buried volume $\%V_{Bur}$ steric parameter (R^2 = 0.9208, Figure 11a). The observed opposite reactivity trends between **1** and **4** are thus originating from the differences in steric hindrance.

Finze and Radius recently developed a LAB-Rep (Lewis Acid/Base Repulsion) model based on the percent buried volumes attributed to both the Lewis acid and base.[23] Applying this model to $B(C_6F_5)_3$,/azatriptycenes **1** and **4** pairs, the $\%V_{Bur\_all}$ values are estimated to range from 93.7% to 96.3% for **1** and from 108.2% to 112.2% for **4**, depending on the selected B-N distance. This outcome is consistent with experimental findings, as the $\%V_{Bur\_all}$ for **1** falls within the lower range of the model, while for **4**, it resides at the upper end of the range.

Moreover, our calculations indicate that the frontier between covalent Lewis adducts and frustrated Lewis pairs is roughly located at a critical pyridine size of $\%V_{Bur}$ (B-N = 1.7 Å) = 37%. This critical size, which corresponds to the $\%V_{Bur}$ of **2**, ($\%V_{Bur}$ = 37.0%), is confirmed experimentally. While the computed ΔG^0 suggests the potential formation of a Lewis adduct (ΔG^0 = -23 kJ mol^{-1}) when **2** is mixed with $B(C_6F_5)_3$, the experiment indicates only a weak interaction with $B(C_6F_5)_3$ similar to **4**. This aligns with the LAB-Rep model, which suggests that the formation of a Lewis adduct with $B(C_6F_5)_3$ is hindered for Lewis bases with $\%V_{Bur}$ between 37 and 42% (falling within the upper range of $\%V_{Bur\_all}$, 105-110%) (see the SI for more details).

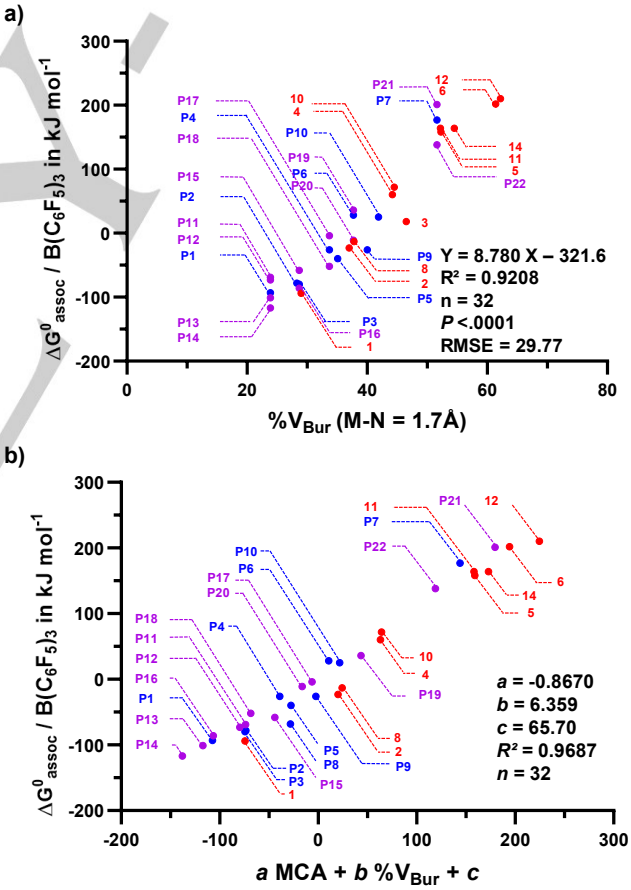

Figure 11. a) Correlation between the $\%V_{Bur}$ (B-N = 1.7 Å) of pyridines and the Gibbs free enthalpies of association ΔG^0 with $B(C_6F_5)_3$. b) Linear relationship between the linear combination of MCA and $\%V_{Bur}$ (B-N = 1.7 Å) and the Gibbs free enthalpies of association ΔG^0 with $B(C_6F_5)_3$ for pyridines. n = sample size, P = *p*-value, and RMSE = root-mean-square error.

A comprehensive correlation matrix detailing the interplay between all steric and electronic parameters (see SI, page S68) is revealing the moderate to good linear correlations between all

parameters, at the exception of the proton affinity (PA), which is fully consistent since no trends are observed between pK_a and Lewis basicity in general.[24a, 24d] The reliable description of the Gibbs free enthalpies ΔG^0 for the complete set of studied pyridines **P1**-**P25** and azatriptycenes **1**-**14** (R^2 = 0.9687) was finally accomplished using a linear multiparametric combination of MCA and $\%V_{Bur}$ descriptors (Figure 11b). These descriptors account for thermodynamic and steric contributions, respectively, and can be used for the future rational prediction of the association of nitrogen Lewis bases with boron Lewis acids.

Conclusion

In conclusion, a series of sterically hindered pyridines based on the triptycene core were synthesized and shown to surpass the size of pyridines known to date. Chiral resolution gave access to enantiopure azatriptycenes, which can open new opportunities in enantioselective catalysis with FLPs and TM-complexes.
The bulkiest azatriptycenes have been used to produce FLPs, while the less sterically hindered have been used as ligands in palladium complexes. The steric properties of a vast array of 2D and 3D pyridine derivatives were determined for the first time based on three widely used steric parameters. Linear correlation between the buried volume parameter related to Lewis acid-base associations $\%V_{Bur}$ (B-N = 1.7 Å), the MCA parameter, and the ΔG^0 values for the association of a wide range of pyridines with $B(C_6F_5)_3$ can be used as a predictive tool for the future design and fine-tuning of new catalysts, showcasing comprehensively the interplay between steric and electronic effects on the reactivity of pyridines. Such structure-properties relationship investigations provide an avenue for the rational use of sterically hindered Lewis bases in catalysis and in predictive reactivity models for catalyst design.

Supporting Information

The authors have cited additional references within the Supporting Information.[32-47]

Acknowledgements

We acknowledge the European Research Council (ERC, B-yond, grant agreement 101044649), the University of Namur and the Fond National de la Recherche Scientifique (F.R.S.-FNRS) for financial support (Grant Numbers: T.0012.21 (G.B), FRIA PhD grant for D.M (1.E.086.20). The calculations were performed on the computers of the Consortium des Équipements de Calcul Intensif en Fédération Wallonie Bruxelles (CÉCI) and particularly those of the Technological Platform of High-Performance Computing, which are supported by the F.R.S.-FNRS, the Walloon Region, the Université de Namur and the Université catholique de Louvain (Conventions No. U.G006.15, U.G018.19, U.G011.22, RW1610468, RW/GEQ2016, RW2110213 and 2.5020.11). We thank the PC2 (UNamur) technological platforms for access to all characterization instruments. RR is a Maître de Recherche of the F.R.S.-FNRS. We thank Prof. Alain Krief and Prof. Sami Lakhdar for their valuable comments on the manuscript.

Keywords: Bulky pyridines • Chiral ligands • Frustrated Lewis pairs • Steric parameters • Pd complexes

[1] a) R. Tandon, T. Unzner, T. A. Nigst, N. De Rycke, P. Mayer, B. Wendt, O. R. P. David, H. Zipse, *Chem. Eur. J.* **2013**, *19*, 6435–6442; b) R. Gujjarappa, N. Vodnala, C. C. Malakar, *ChemistrySelect* **2020**, *5*, 8745–8758.

[2] a) G. Höfle, W. Steglich, H. Vorbrüggen, *Angew. Chem. Int. Ed. in English* **1978**, *17*, 569–583; b) C. Grondal, *Synlett* **2003**, *2003*, 1568–1569; c) N. D. Rycke, G. Berionni, F. Couty, H. Mayr, R. Goumont, O. R. P. David, *Org. Lett.* **2011**, *13*, 530–533.

[3] a) S. J. Geier, D. W. Stephan, *J. Am. Chem. Soc.* **2009**, *131*, 3476–3477; b) D. Winkelhaus, B. Neumann, H.-G. Stammler, N. W. Mitzel, *Dalton Trans.* **2012**, *41*, 9143–9150; c) C. B. Caputo, S. J. Geier, D. Winkelhaus, N. W. Mitzel, V. N. Vukotic, S. J. Loeb, D. W. Stephan, *Dalton Trans.* **2012**, *41*, 2131–2139; d) Y. Liu, H. Du, *J. Am. Chem. Soc.* **2013**, *135*, 6810–6813; e) L. Greb, C.-G. Daniliuc, K. Bergander, J. Paradies, *Angew. Chem. Int. Ed.* **2013**, *52*, 5876–5879; f) E. R. Clark, M. J. Ingleson, *Angew. Chem. Int. Ed.* **2014**, 53, 11306–11309; g) L. A. Körte, R. Warner, Y. V. Vishnevskiy, B. Neumann, H.-G. Stammler, N. W. Mitzel, *Dalton Trans.* **2015**, *44*, 9992–10002; h) U. Gellrich, *Angew. Chem. Int. Ed.* **2018**, 57, 4779–4782; i) J. Paradies, *Coord. Chem. Rev.* **2019**, *380*, 170–183; j) F. Wech, M. Hasenbeck, U. Gellrich, *Chem. Eur. J.* **2020**, *26*, 13445–13450.

[4] a) M. N. Zafar, A. H. Atif, M. F. Nazar, S. H. Sumrra, Gul-E-Saba, R. Paracha, *Russ J Coord Chem* **2016**, *42*, 1–18; b) A. Mishra, R. Gupta, *Dalton Trans.* **2014**, *43*, 7668–7682.

[5] C. J. O'Brien, E. A. B. Kantchev, C. Valente, N. Hadei, G. A. Chass, A. Lough, A. C. Hopkinson, M. G. Organ, *Chem. Eur. J.* **2006**, *12*, 4743–4748.

[6] J. A. Love, J. P. Morgan, T. M. Trnka, R. H. Grubbs, *Angew. Chem. Int. Ed.* **2002**, *41*, 4035–4037.

[7] H.-L. Kwong, H.-L. Yeung, C.-T. Yeung, W.-S. Lee, C.-S. Lee, W.-L. Wong, *Coord. Chem. Rev.* **2007**, *251*, 2188–2222.

[8] a) J. C. Ruble, G. C. Fu, *J. Org. Chem.* **1996**, *61*, 7230–7231. b) G. C. Fu, *Acc. Chem. Res.* **2000**, *33*, 412–420; c) R. Rios, J. Liang, M. M.-C. Lo, G. C. Fu, *Chem. Commun.* **2000**, 377–378; d) G. C. Fu, *Acc. Chem. Res.* **2004**, *37*, 542–547; e) M. Ogasawara, S. Wada, E. Isshiki, T. Kamimura, A. Yanagisawa, T. Takahashi, K. Yoshida, *Org. Lett.* **2015**, *17*, 2286–2289; f) O. Bernardo, S. González-Pelayo, L. A. López, *Eur. J. of Inorg. Chem.* **2022**, *2022*, e202100911.

[9] U. Wörsdörfer, F. Vögtle, F. Glorius, A. Pfaltz, *Journal für praktische Chemie* **1999**, *341*, 445–448.

[10] N. Takenaka, R. S. Sarangthem, B. Captain, *Angew. Chem. Int. Ed.* **2008**, *47*, 9708–9710.

[11] J. Wang, M.-W. Chen, Y. Ji, S.-B. Hu, Y.-G. Zhou, *J. Am. Chem. Soc.* **2016**, *138*, 10413–10416.

[12] P. Song, L. Hu, T. Yu, J. Jiao, Y. He, L. Xu, P. Li, *ACS Catal.* **2021**, *11*, 7339–7349.

[13] M. Charton, B. Charton, *J. Am. Chem. Soc.* **1975**, *97*, 6472–6473.

[14] A. Verloop, W. Hoogenstraaten, J. Tipker, in *Drug Design* (Ed.: E.J. Ariëns), Academic Press, Amsterdam, **1976**, pp. 165–207.

[15] C. A. Tolman, *Chem. Rev.* **1977**, *77*, 313–348.

[16] a) A. C. Hillier, W. J. Sommer, B. S. Yong, J. L. Petersen, L. Cavallo, S. P. Nolan, *Organometallics* **2003**, *22*, 4322–4326; b) H. Clavier, S. P. Nolan, *Chem. Commun.* **2010**, *46*, 841–861; c) L. Falivene, Z. Cao, A.

Petta, L. Serra, A. Poater, R. Oliva, V. Scarano, L. Cavallo, *Nat Chem* **2019**, *11*, 872–879.

[17] a) N. Fey, A. C. Tsipis, S. E. Harris, J .N. Harvey, A. G. Orpen, R. A. Mansson, *Chem. Eur. J.* **2006**, *12*, 291−302; b) J. Jover, N. Fey, J. N. Harvey, G. C. Lloyd-Jones, A. G. Orpen, G. J. J. Owen-Smith, P. Murray, D. R. J. Hose, R. Osborne, M. Purdie, *Organometallics* **2012**, *31*, 5302–5306.

[18] a) A. Poater, F. Ragone, R. Mariz, R. Dorta, L. Cavallo, *Chem. Eur. J.* **2010**, *16*, 14348–14353; b) L. Falivene, R. Credendino, A. Poater, A. Petta, L. Serra, R. Oliva, V. Scarano, L. Cavallo, *Organometallics* **2016**, *35*, 2286–2293.

[19] a) K. C. Harper, E. N. Bess, M. S. Sigman, *Nature Chem* **2012**, *4*, 366–374; b) B. Pinter, T. Fievez, F. M. Bickelhaupt, P. Geerlings, F. D. Proft, *Phys. Chem. Chem. Phys.* **2012**, *14*, 9846–9854; c) D. J. Durand, N. Fey, *Chem. Rev.* **2019**, *119*, 6561–6594.

[20] a) A. L. Seligson, W. C. Trogler, *J. Am. Chem. Soc.* **1991**, *113*, 2520–2527; b) J. A. Bilbrey, A. H. Kazez, J. Locklin, W. D. Allen, *Journal of Computational Chemistry* **2013**, *34*, 1189–1197.

[21] C. Jiang, O. Blacque, T. Fox, H. Berke, *Organometallics* **2011**, *30*, 2117–2124.

[22] J. A. Denny, M. Y. Darensbourg, *Coord. Chem. Rev.* **2016**, *324*, 82–89.

[23] L. Zapf, M. Riethmann, S. A. Föhrenbacher, M. Finze, U. Radius, *Chem. Sci.* **2023**, *14*, 2275–2288.

[24] a) H. Mayr, J. Ammer, M. Baidya, B. Maji, T. A. Nigst, A. R. Ofial, T. Singer, *J. Am. Chem. Soc.* **2015**, *137*, 2580–2599; b) E. Follet, H. Zipse, S. Lakhdar, A. R. Ofial, G. Berionni, *Synthesis* **2017**, *49*, 3495–3504; c) R. J. Mayer, N. Hampel, A. R. Ofial, *Chem. Eur. J.* **2021**, *27*, 4070–4080; d) M. Orlandi, M. Escudero-Casao, G. Licini, *J. Org. Chem.* **2021**, *86*, 3555–3564.

[25] a) E. Bosch, C. L. Barnes, *Inorg. Chem.* **2001**, *40*, 3234–3236; b) T. Pell, D. P. Mills, A. J. Blake, W. Lewis, S. T. Liddle, *Polyhedron* **2010**, *29*, 120–125; c) J. Schröder, D. Himmel, T. Böttcher, *Chem. Eur. J.* **2017**, *23*, 10763–10767.

[26] a) G. Preda, A. Nitti, D. Pasini, *ChemistryOpen* **2020**, *9*, 719–727. b) Md. N. Khan, T. Wirth, *Chem. Eur. J.* **2021**, *27*, 7059–7068. c) K. Nikitin, H. Müller-Bunz, Y. Ortin, J. Muldoon, M. J. McGlinchey, *J. Am. Chem. Soc.* **2010**, *132*, 17617–17622. d) R. Inoue, K. Furumoto, Y. Morisaki, *Chem. Commun.* **2023**, *59*, 5571–5574. e) D. Moser, T. A. Schmidt, C. Sparr, *JACS Au* **2023**, *3*, 2612–2630.

[27] J. H. Markgraf, H. A. Davis, P. S. Ernst, K. S. Hirsch, K. J. Leonard, M. E. Morrison, C. R. Myers, *Tetrahedron* **1991**, *47*, 183–188.

[28] a) T. Satoh, J. Shishikura, Y. Hayashi, K. Yamakawa, *Chem. Lett.* **1992**, *21*, 381–384. b) K. Lehr, R. Mariz, L. Leseurre, B. Gabor, A. Fürstner, *Angew. Chem. Int. Ed* **2011**, *50*, 11373–11377.

[29] P. Beak, A. I. Meyers, *Acc. Chem. Res.* **1986**, *19*, 356–363.

[30] H. Mayr, J. Ammer, M. Baidya, B. Maji, T. A. Nigst, A. R. Ofial, T. Singer, *J. Am. Chem. Soc.* **2015**, *137*, 2580–2599. b) H. Mayr, A. R. Ofial, *Acc. Chem. Res.* **2016**, *49*, 952-965.

[31] a) F. Brotzel, B. Kempf, T. Singer, H. Zipse, H. Mayr, *Chem. Eur. J.* **2007**, *13*, 336–345. b) E. Follet, H. Zipse, S. Lakhdar, A. R. Ofial, G. Berionni, *Synthesis* **2017**, *49*, 3495–3504.

[32] V. Fasano, A. W. McFord, C. P. Butts, B. S. L. Collins, N. Fey, R. W. Alder, V. K. Aggarwal, *Angew. Chem. Int. Ed.* **2020**, *59*, 22403–22407.

[33] C. Wang, D. M. Flanigan, L. N. Zakharov, P. R. Blakemore, *Org. Lett.* **2011**, *13*, 4024–4027.

[34] A. Wasilewska, B. A. Woźniak, G. Doridot, K. Piotrowska, N. Witkowska, P. Retailleau, Y. Six, *Chem. - Eur. J.* **2013**, *19*, 11759–11767.

[35] C. Zhu, Y. Zhao, D. Wang, W.-Y. Sun, Z. Shi, *Sci. Rep.* **2016**, 6, 33131.

[36] a)V. Lisowski, M. Robba and S. Rault, *J. Org. Chem.*, **2000**, *65*, 4193. b) M. Barbero, S. Cadamuro, S. Dughera and R. Torregrossa, *Org. Biomol. Chem.*, **2014**, *12*, 3902. c) C. S. Buxton, D. C. Blakemore, J. F. Bower, *Angew. Chem., Int. Ed.* **2017**, *56*, 13824.

[37] X. Qiao, M. A. Padula, D. M. Ho, N. J. Vogelaar, C. E. Schutt, R. A. Pascal, Jr., *J. Am. Chem. Soc.* **1996**, *118*, 741.

[38] Deposition numbers 1164754 ; 186689 ; 1819429 ; 678772 ; 105738 ; 1160020 ; 105736 ; 105737 ; 1500171 ; 1474206 ; 1889212 ; 867944 ; 940291 ; 940290 ; 738299 ; 228833 ; 601622 ; 742849 ; 1506903 ; 837204 ; 855568 ; 1500163 ; 677127 ; 132231 ; 267654 ; 1042287 ; 655973 ; 1500169 ; 835253 ; 1500158 ; 1102653 ; 2064616 ; 172578 ; 1984259 ; 1034733 ; 1453484 ; 1453485 ; 766550 ; 2019884 ; 1530723 ; 1294939 ; 790881 ; 742848 ; 2013898 ; 2013898 ; 2059582 ; 1102795 ; 1120495 ; 637580 ; 709095 ; 672396 ; 178251 ; 852841 ; 613508 ; 923003 ; 837205 ; 908969 ; 613510 ; 655973 ; 835253 ; 837205 ; 908968 ; 2006099 ; 2201289 ; 2064616 ; 917003 ; 766549 ; 1103401 ; 1990786 ; 728406 ; 728404 ; 1892837 ; 1855212 ; 1855213 ; 858889 ; 728403 ; 1296785 ; 1551359 ; 168864 ; 224547 ; 189487 ; 1100987 ; 613446 ; 138392 ; 1002447 ; 673034 ; 771412 ; 1100459 ; 168836 ; 699539 ; 1453916 ; 767868; 1455885 ; 801515 ; 694400 ; 694398 ; 694399 contain the supplementary crystallographic data for this paper. These data are provided free of charge by the joint Cambridge Crystallographic Data Centre and Fachinformationszentrum Karlsruhe Access Structures service.

[39] J. Vrána, M.A. Samsonov, V. Němec, A. Růžička, *Chem. Commun.* **2020**, 56, 2–5.

[40] C.A. Tolman, *J. Am. Chem. Soc.* **1970**, *92*, 2956.

[41] M. J. Frisch, G. W. Trucks, H. B. Schlegel, G. E. Scuseria, M. A. Robb, J. R. Cheeseman, G. Scalmani, V. Barone, G. A. Petersson, H. Nakatsuji, X. Li, M. Caricato, A. V. Marenich, J. Bloino, B. G. Janesko, R. Gomperts, B. Mennucci, H. P. Hratchian, J. V. Ortiz, A. F. Izmaylov, J. L. Sonnenberg, D. Williams-Young, F. Ding, F. Lipparini, F. Egidi, J. Goings, B. Peng, A. Petrone, T. Henderson, D. Ranasinghe, V. G. Zakrzewski, J. Gao, N. Rega, G. Zheng, W. Liang, M. Hada, M. Ehara, K. Toyota, R. Fukuda, J. Hasegawa, M. Ishida, T. Nakajima, Y. Honda, O. Kitao, H. Nakai, T. Vreven, K. Throssell, J. A. Montgomery, Jr., J. E. Peralta, F. Ogliaro, M. J. Bearpark, J. J. Heyd, E. N. Brothers, K. N. Kudin, V. N. Staroverov, T. A. Keith, R. Kobayashi, J. Normand, K. Raghavachari, A. P. Rendell, J. C. Burant, S. S. Iyengar, J. Tomasi, M. Cossi, J. M. Millam, M. Klene, C. Adamo, R. Cammi, J. W. Ochterski, R. L. Martin, K. Morokuma, O. Farkas, J. B. Foresman, D. J. Fox, *Gaussian 16, Revision A.03*, Gaussian Inc., Wallingford CT, **2016**.

[42] Y. Zhao, D. G. Truhlar, *Theor. Chem. Acc.* **2008**, 120, 215-241.

[43] F. Weigend, R. Ahlrichs, *Phys. Chem. Chem. Phys* **2005**, 7, 3297-3305.

[44] D. Mahaut, A. Chardon, L. Mineur, G. Berionni, B. Champagne, *ChemPhysChem* **2021**, 22, 1958-1966.

[45] J. Tomasi, B. Mennucci, R. Cammi, *Chem. Rev.* **2005**, 105, 2999-3094.

[46] N. Fey, J. N. Harvey, G. C. Lloyd-Jones, P. Murray, A. G. Orpen, R. Osborne, M. Purdie, *Organometallics* **2008**, *27*, 1372–1383.

[47] Jaguar 8.5, Schrodinger, Inc., New York, NY, **2014.**

RESEARCH ARTICLE

Highly sterically hindered chiral pyridines were synthesized and resolved by HPLC. Their Brønsted/Lewis basicity were evaluated, and their reactivity was studied through their combination with Pd and $B(C_6F_5)_3$ to generate new types of ligands/frustrated Lewis pairs. The study involved the first parameterization of the steric hindrance for a large set of pyridine derivatives.

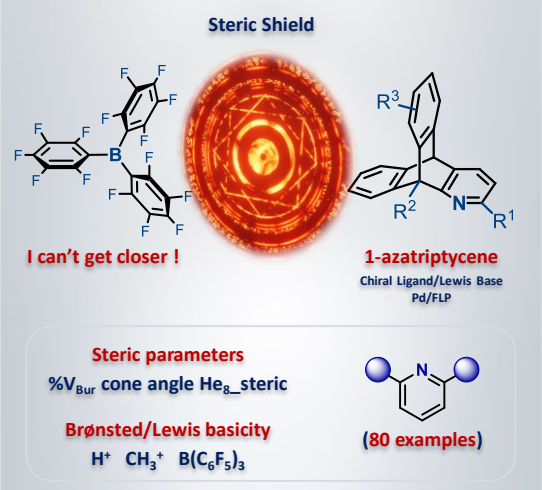

*Ali Ben Saida, Damien Mahaut, Nikolay Tumanov, Johan Wouters, Benoît Champagne, Nicolas Vanthuyne, Raphaël Robiette, Guillaume Berionni**

Page No. – Page No.

Reactivity and Steric Parameters from 2D to 3D Bulky Pyridines : Increasing Steric Demand at Nitrogen with Chiral Azatriptycenes